Skin biological responses to urban pollution in an ex vivo model

Angela Patatian, Charlène Delestre-Delacour, Guiseppe Percoco, Yasmina Ramdani, Marine Di Giovanni, Laurent Peno-Mazzarino, Thomas Bader, Magalie Bénard, Azeddine Driouich, Elian Lati, et al.

Skin biological responses to urban pollution in an *ex vivo* model

Patatian A.[a]*[£], Delestre-Delacour C.[b]*, Percoco G.[c], Ramdani Y.[b], Di Giovanni M.[e], Peno-Mazzarino L.[c], Bader Th.[a], Bénard M.[e], Driouich A.[b,d,e], Lati E.[a, c], Benech P.[a,f]#, and Follet-Gueye M.L.[b, d,e]#[£]

[a]**Laboratoire GENEX,** 91160 Longjumeau, France

[b]**Laboratoire de Glycobiologie et Matrice Extracellulaire Végétale (GlycoMEV)** EA4358, Université de Rouen Normandie, 76821 Mont-Saint-Aignan, France

[c]**Laboratoire BIO-EC**, 91160 Longjumeau, France

[d]Fédération de Recherche «Normandie Végétal » -FED 4277-76000, Rouen, France

[e]**Plate-Forme de Recherche en Imagerie Cellulaire (PRIMACEN**), Université de Rouen Normandie, 76821 Mont-Saint-Aignan, France

[f]**Aix Marseille Université,** CNRS, INP, UMR 7150, 13916 Marseille, France

* *Equal contribution*

\# *-Senior Co-authors*

£Corresponding author: marie-laure.follet-gueye@univ-rouen.fr

£Corresponding author: a.patatian@laboratoire-genex.fr

ABSTRACT

The skin epidermis is continuously exposed to external aggressions, including environmental pollution. The cosmetic industry must be able to offer dedicated products to fight the effects of pollutants on the skin. We set up an experimental model that exposed skin explants maintained in culture to a pollutant mixture. This mixture representing urban pollution was designed on the basis of the French organization 'Air Parif' database. A chamber, called Pollubox®, was built to allow a controlled nebulization of P on the cultured human skin explants. We investigated ultrastructural morphology by transmission electron microscopy of high pressure frozen skin explants. ~~At first, we detected by transmission electron microscopy some matters smaller than 300 nm similar to diesel particles in the granular layer of the epidermis.~~ A global transcriptomic analysis indicated that the pollutant mixture was able to induce relevant xenobiotic and antioxidant responses. Modulated detoxifying genes were further investigated by laser micro-dissection coupled to qPCR, and immunochemistry. Both approaches showed that P exposure correlated with overexpression of detoxifying genes and provoked skin physiological alterations down to the *stratum basale*. The model developed herein might be an efficient tool to study the effects of pollutants on skin as well as a powerful testing method to evaluate the efficacy of cosmetic products against pollution.

Keywords : environmental pollution, *ex vivo* skin, transcriptomic, xenobiotic response, laser capture micro-dissection, transmission electron microscopy

1. INTRODUCTION

Nowadays, urban air pollution is known to be a major threat to health and environment. The World Health Organization (WHO) reported that in 2016, 91% of the world population was living in places where the WHO air quality guidelines were not met. Moreover, outdoor air pollution in both cities and rural areas was estimated to cause 4.2 million premature deaths worldwide in 2016. This mortality is due to exposure to small particulate matter of 2.5 µm or less in diameter which causes cardiovascular and respiratory diseases and cancer. Increasing urbanization enhances particulate matter content in the atmosphere as wells as the level of several other pollutants such as polycyclic aromatic hydrocarbons and heavy metals. Effect of urban air pollutant exposure on the lung physiology has been largely described but little is known about those impacts on the skin (Estrella et al. 2019).

Epidermis, as the outermost line of defense of our organism is continuously exposed to a vast range of stressors, including ultraviolet radiations and atmospheric pollutants. Skin ageing related to pollutant or UV radiation exposures has been clearly established (Vierkötter et al. 2010). Repeated stimulations of protective processes in skin seem to induce skin ageing (Estrella et al. 2019). The negative impact of environmental pollution on skin microbiota composition has been also described (Jo et al. 2017). Moreover, pore obstruction by particulate matter is able to enhance the formation of an anaerobic environment, which leads to the proliferation of *Propionibacterium acnes*, contributing to acne development. At a molecular level, pollutants trigger the activation of Aryl hydrocarbon Receptor (AhR) that is involved in the detoxification process (Denison and Nagy 2003; Iyanagi 2007). This chemosensor molecule is found in various types of tissues including the skin where it mediates the xenobiotic response and modulates cell proliferation, inflammation and melanogenesis (Abel and Haarmann-Stemmann 2010). Following stimulation, AhR translocates to the nucleus of the cell where it interacts with AhR nuclear translocator

(ARNT) and binds the Xenobiotic Response Element (XRE) DNA domain to initiate the transcription of genes involved in cell detoxification (Sonoda et al. 2003). Although this process is considered as a protective response against toxic compounds, its sustained activation upon repeated exposures can be deleterious and might be responsible for skin alterations (Mancebo and Wang 2015). For instance, among AhR target genes, cytochrome P450 is responsible for the production of reactive oxygen species (ROS) (Denison and Nagy 2003; Hirabayashi 2005). The control of ROS is crucial for cellular homeostasis. An excessive ROS production can cause DNA and protein damages as well as lipid peroxidation that alters the barrier function and consequently skin hydration (Rhee 2006; Addor 2017). The resulting redox imbalance leads to an antioxidant response involving the NRF2 pathway. As a transcription factor, NRF2 binds the Antioxidant Response Element DNA domain (ARE) to promote the transcription of genes involved in antioxidant processes (Jackson et al. 2015). NRF2 activation may be one way to avoid chronic inflammation through the decrease of oxidative stress (Kurutas 2016).

Most of the investigations launched to study the impact of pollutants on skin physiology were based mainly on *in vitro* studies using primary cells such as keratinocytes, fibroblasts or immortalized human cell lines (HaCaT) (Min-Duk Seo et al. 2012 ; Binelli et al. 2018; Zhang et al. 2017). These cellular models lack the high biological complexity that characterizes the human's biggest organ which is the skin. Cell culture cannot take into account the cross-talk between distinct cell types and skin appendages such as hair follicles, apocrine and eccrine sweat glands required to reflect the activities of the cutaneous tissue. Most previous studies in this field were conducted using a single pollutant rather than a mix of different pollutants like it is the case under real conditions (Kazi et al. 2008; Philips et al. 2010). These limitations can be considered as a brake to study the impact of pollutants on skin, and for the development by the cosmetic industries of protective or regenerative products. Herein we present an

experimental model that relies on the use of human skin explants. In contrast to cultured cells and reconstructed epidermis, explants contain all resident cell types of the epidermis and dermis as well as skin appendages and can be cultured under air-liquid interface conditions for up to 10-12 days (Gasser et al. 2008). Thus, this *ex vivo* model constitutes an interesting alternative although skin explants stem from surgical tissues of donors and might differ in some biological processes or responses due to their genetic variability. Therefore, explants were used to see whether or not they could respond to pollutant exposure and serve as the basis of a test to evaluate anti-pollutant activities of cosmetic ingredients or products. To achieve experimental conditions as close as possible to reality, a pollutant mixture was designed according to the French non-profit organization 'Air Parif' and nebulized on the cultured human skin explants (HSE) within a dedicated chamber, the Pollubox®. Using this tool, only the *stratum corneum* (SC) was directly exposed to pollutants. Transmission electron microscopy (TEM) observations of high-pressure frozen HSE after pollutant exposure allowed the visualization ~~of some matter similar to diesel particles in the epidermis and~~ of an increase in the number of extracellular vesicles (EV) like structures, which are known to be involved in cell communication (Carrasco et al., 2019). Furthermore, gene expression analyses using whole genome microarrays showed that our experimental conditions were able to elicit a xenobiotic and antioxidant responses as well as to modulate genes involved in skin barrier homeostasis. Although the extent of such a modulation varied according to the donors, the expression of skin barrier-related genes was consistently found most affected. RT-qPCR performed on RNA extracted after laser capture micro dissection demonstrated that the level of induction was higher in the basal layers than in the granular layers. Altogether, these results supported that our experimental device can be efficient to test cosmetic ingredients or end products for their ability to counteract the effects of pollutants.

MATERIALS & METHODS

2.1 Preparation of human skin explants

BIO-EC Laboratory possesses an authorization from the Bioethics group of the general director services of the French research and innovation ministry (registered under n°DC-2008-542) to use human skin from surgical waste since 5th May 2010.

The study was performed in accordance with the Declaration of Helsinki after the patients had given informed consent to use their skin samples by BIO-EC Laboratory.

Full-thickness human skin biopsies were obtained from abdomen of healthy female donors who had undergone plastic surgery. The hypodermis was removed from the skin and circular explants (~1 cm diameter, 0.2 cm thickness and ~200 mg weight) were excised using a sample punch. Samples were placed immediately in BIO-EC's Explant Medium (BEM). From day 1 they were cultured under classical cell culture conditions (37°C in 5% CO_2). Table S1 summarizes the different experiments completed during our study on the HSE from various volunteers in the context of the URBASKIN project supported by the French FUI *(Fonds Unique Interministériel).*

2.2 Air pollutant exposure

In order to develop the experimental conditions, several concentrations of pollutant mix (P) were evaluated. The pollutants were dissolved in nitric acid (Merck, 1.00441.0250), ethanol (VWR, 20281.467), and DMSO (Sigma-Aldrich, 47231), as indicated in Table S2.

The dose of P, which can induce physiological modifications at the molecular level after nebulization at 5 different doses (expressed in mg/m^3 or in µg/ml) on HSE, was evaluated by RT-qPCR quantification of stress marker gene expression (CYP1A1, GPX2, HMOX1, and SQSTM1) comparing P versus organic solvent (OS) (Figure S1B). Induction of all evaluated genes was observed after 24h of exposure to the highest dose (P1) among those tested, corresponding to 100 000 mg/m^3 (Figure S1A). Therefore this dose was chosen for all further

investigations. The explants from the same donor were placed in BEM for 5 days before being transferred to the Pollubox® and nebulized with 3 ml of P for 1h30 at the different selected doses.

The Pollubox® device (Figure S2) is an exposure chamber designed by BIO-EC laboratory. The system is composed of a chamber and a basis both made of poly (methyl methacrylate) resin.

The basis contains 12 holes with a diameter of 8 mm restricting the exposure to the skin explant surface alone. For the exposure to pollutants, skin explants are placed in a classical 12-well cell culture plate with 1 ml of BEM (BIO-EC culture medium) per well. The culture plate is then positioned under the basis of the Pollubox® in order to align skin explants at the levels of the holes of the basis. A nebulizer (Aerogen Pro®), placed on the top of the chamber, allows to nebulize the liquid solution containing the pollutants. The generated aerosol precipitates uniformly on the surface of skin explants placed at the basis of the Pollubox®, avoiding any systemic contamination of the samples.

HSE controls received the mix of OS used to solubilize the pollutants. The final concentrations of OS were: Nitric acid 1.7% (v/v), DMSO 8.5% (v/v) and ethanol 4% (v/v). For transcriptomic study (microarray or qPCR), HSE were harvested 24h after P or OS exposure. For immunostaining studies and general morphology evaluation by optical and transmission electron microscopies, HSE were harvested 48h after P and OS exposure. For ~~diesel particle penetration analysis by~~ tape-stripping assay (see § 2.8), skin explants were treated in the Pollubox® with a solution containing diesel particles at 0.1% dissolved in OS and sampled 24 hours later.

2.3 Sampling

On day 0, 3 explants from the batch T0 were collected and cut in 3 parts: one third was frozen at -80°C for immunostaining, another third was fixed in formol solution for evaluation of the

skin morphology, and the third part was preserved in RNAlater (Qiagen, 76106) for the transcriptomic study. On day 6 and day 7, respectively, 24h and 48h after pollutant exposure, skin explants were processed in the same way as on day 0.

2.4 Optical microscopy analysis

The observation of the general morphology was evaluated after staining of formol-fixed paraffin-embedded (FFPE) skin sections according to Masson's trichrome protocol, Goldner variant. The primary antibodies used in immunohistochemistry are listed in Table S3.

For all the primary antibodies, a pre-diluted horse serum (Vector laboratories, ref. PK7200) and a universal horse secondary antibody were used (Vector laboratories, ref. PK7200).

All the microscopical observations were performed using a Leica DMLB or a BX43 Olympus microscope. Pictures were digitized with an Olympus DP72 camera and the Cell^D data storing software.

2.5 Gene Expression Profile

Total RNAs were extracted from skin explants using the ReliaPrep Tissue Miniprep kit (Promega Z6111) after mechanical disruption and homogenization by TissueLyser (Qiagen). RNAs (70ng) of each explant from 4 donors (V1 to V4 in Table S1) were used for reverse transcription, amplification and Cy3 labeling, using the Low Input Labeling kit, one-color (Agilent Technologies). All cRNAs were hybridized to human whole genome oligo microarrays (Agilent Technologies V3 AMADID072363), which contains 60.000 probes, derived from the National Center for Biotechnology Information Reference Sequence (NCBI) RefSeq. Microarray data were quantified (GeneExtraction Feature V10.7) and normalized with R tools (Bioconductor) and deposited in the public domain (GEO Submission GSE126440). Subsequently, fold-changes (FC) (Table S4) were deduced from the calculated ratios: gene intensity of treated samples by P *versus* gene intensity of control samples treated by OS. 79 upregulated genes were selected for a FC≥1.45 and 68 downregulated genes for a

FC≤0.65. Only annotated genes presenting intensity values ≥50 (that included those higher than background) for treated conditions were conserved in our analysis.

Selected genes were subjected to functional analysis by PredictSearch® in order to identify the induced biological effects. PredictSearch® is a powerful text mining software that identifies correlations between genes and biological processes/diseases across all scientific publications cited in the PubMed database (Benech and Patatian 2014; Eyles et al. 2007; Michel et al. 2017).

2.6 Term enrichment analysis

Terms related to the set of genes modulated by P were issued from PredictSearch® analysis according to their p-values. For each term, the ratio (C=A/B) represents the number of term-related genes (A) among the number of selected genes (B). This calculation was compared to the ratio (F=D/E) representing the number of term-related genes (D) among all the 20 080 genes (E) contained in the PredictSearch® Database. The ratio (I=C/F) provides an enrichment value that was further normalized through the calculation of a ratio (K=J/F) based on the ratio (J=G/H) representing the number of term-related genes (G) among a set of randomly chosen genes (H) of the same size than the set of our gene selection (B) compared again to the F ratio. This new ratio (K) is then compared to the I ratio to give a normalized enrichment score (NES) defined by the I/K ratio.

2.7 Laser capture micro-dissection (LCM), RNA extraction from micro-dissected explants and real-time qPCR

According to Percoco et al. (2012), the *stratum granulosum* (SG) and the *stratum basale* (SB) of the epidermis were micro-dissected by LCM and total RNAs were extracted using an RNeasy Micro kit (Qiagen) following the manufacturer's instructions. The quality and quantity of the RNAs were assessed by microfluidic capillary electrophoresis (Agilent 2100 Bioanalyzer, Agilent Technologies). Amplification reactions were performed using a

QuantStudio 12K Flex Real-time PCR System (Applied Biosystems). When possible, intron-spanning primers were designed using Primer Express 3.0.1 software (Applied Biosystems; Table S6).

2.8 Tape-stripping experiment

A D-Squame® disc with a 14 mm diameter (D101, CuDerm), was used (24h after Pollubox® exposure) to remove corneocytes from 3 skin explants (from donor V10; Table S1) exposed or not to diesel particle-enriched solution (diluted at 0.1% in OS) in the Pollubox®. The disc covering the entire surface of the skin explants was successively applied 10 times and was then fixed for 30 min at 4°C in a solution of 2% glutaraldehyde. After post-fixation in 1% OsO_4 for 1h at 4°C, it was embedded in 3% low melting point agarose. Samples were dehydrated as follows: 35% ethanol for 10 min; 70% ethanol for 3 min; 100 % ethanol for 1 min. Infiltration was carried out at room temperature in London Resin White (LRW, EMS) for 30 min. Polymerization was performed at 60°C for 24h. Ultrathin sections (70 nm) were collected on formvar carbon-coated nickel grids, stained with UranyLess solution and lead citrate solution (Delta microscopies). Observations were performed with a Philips Tecnai 12 Biotwin FEI transmission electron microscope (Philips).

2.9 High pressure freezing (HPF) and freeze substitution (FS)

For ultrastructural and immunogold analyses, 48h after Pollubox® exposure, triplicate skin explants from a healthy 39-year-old Caucasian women (donor V4, table S1), exposed to OS or P in the Pollubox®, were cryofixed by HPF as previously described (Percoco et al. 2013). Briefly, specimens were cut into small discs (≈3 mm in diameter and 300 µm thick) and cryofixed in a high-pressure freezer (HPM100, Leica). After high pressure freezing, samples were cryosubstituted with the automate freeze substitution (AFS-FSP, Leica) and embedded in LRW resin as described by Percoco et al. (2013). Ultrathin sections (70 nm) were processed and observed as mentioned in § 2.8.

2.10 Immunogold labeling

Ultrathin sections of skin explants were treated with 0.1M glycine for 10 min and incubated for 30 min with 10% normal goat serum (NGS) in PBS + 0.1% Tween 20 + 1% BSA. Samples were incubated with primary and secondary antibodies as follows: 1h at 25°C, mouse-anti-AhR (1/5; MA1-514, Thermo Fischer; Table S3) in saturation buffer (0.1% Tween 20 + 1% BSA + 1% NGS in PBS); goat anti-mouse antibody coupled to 25 nm gold particles (1/20; Aurion) in PBS + 0.005% Tween 20.

2.11 Statistical analysis

A Two-way ANOVA (R, Mkmisc package) was performed for p-values (Pval) evaluation using a design based on each probe including treatment factor (P vs OS) and volunteer factors (V1-V2-V3-V4) in order to take into account the heterogeneity between volunteers. For fold-change computing (P vs OS) we applied the same design using the removeBatchEffect function from the Limma package. Only p-values (P) less than 0.05 were considered significant.

The ratio of gene expression between OS and P treatment in SB and SG enriched fractions was determined with the ΔΔCt method and were calculated using the OS expression profile as a reference. First, the Shapiro-Wilk normality test allowed to determine which data followed a normal distribution. In case of a Gaussian distribution, the data were analyzed statistically by unpaired t-test with Welch's correction if variances were non-equal (GraphPad PRISM v7.0, GraphPad Software Inc). In case of a non-Gaussian distribution, the data were analyzed using the Mann-Whitney test (*P <0.1; ** P <0.05). All data were shown as mean ± SEM calculated from three independent experiments.

2. RESULTS AND DISCUSSION

To investigate the skin alterations that might be caused by a pollution mixture, we combined different molecules according to the French non-profit organization 'Air Parif' (Table S2). The resulting pollutant mixture (P) was nebulized on the cultured explants into a dedicated chamber, the Pollubox® (Figure S2). A mixture of the different OS used to solubilize the pollutants served as control (Table S2). The impacts of P either on skin morphology, or on gene and protein expression were investigated on skin explants originating from several donors (Table S1). The optimal dose allowing the detection of an effective cutaneous response to pollutant stress was determined through the evaluation of the induced expression of genes well known to be involved in the detoxification process such as *CYP1A1*, *GPX2*, *HMOX1*, and *SQSTM1* (Figure S1).

3.1 Effect of pollutant exposure on skin morphology

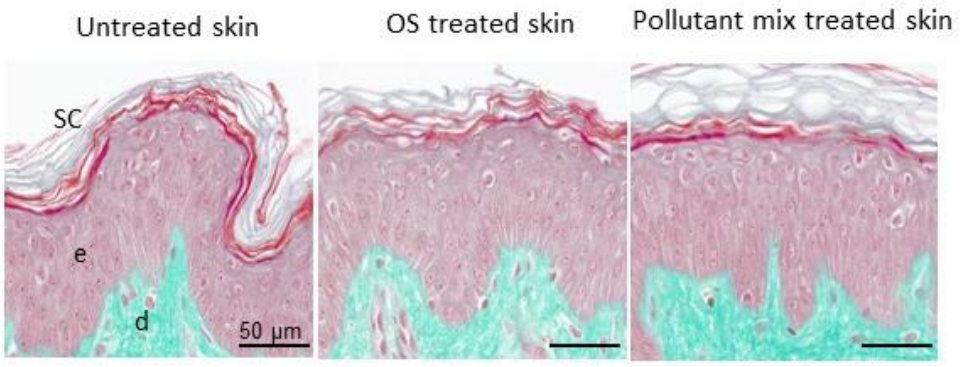

Figure 1: Skin morphology 48 h after pollutant mix exposure.
General morphology was analyzed on FFPE skin sections stained using Masson's trichrome protocol. e, epidermis; d, dermis; OS, organic solvent; SC, *stratum corneum*. Scale bars: 50 µm.

P exposure did not lead to global skin morphology alterations (Figure 1). Nevertheless, TEM analysis on explants treated with P revealed an increase of extracellular vesicle (EV)-like structures in the epidermis (Figure 2).

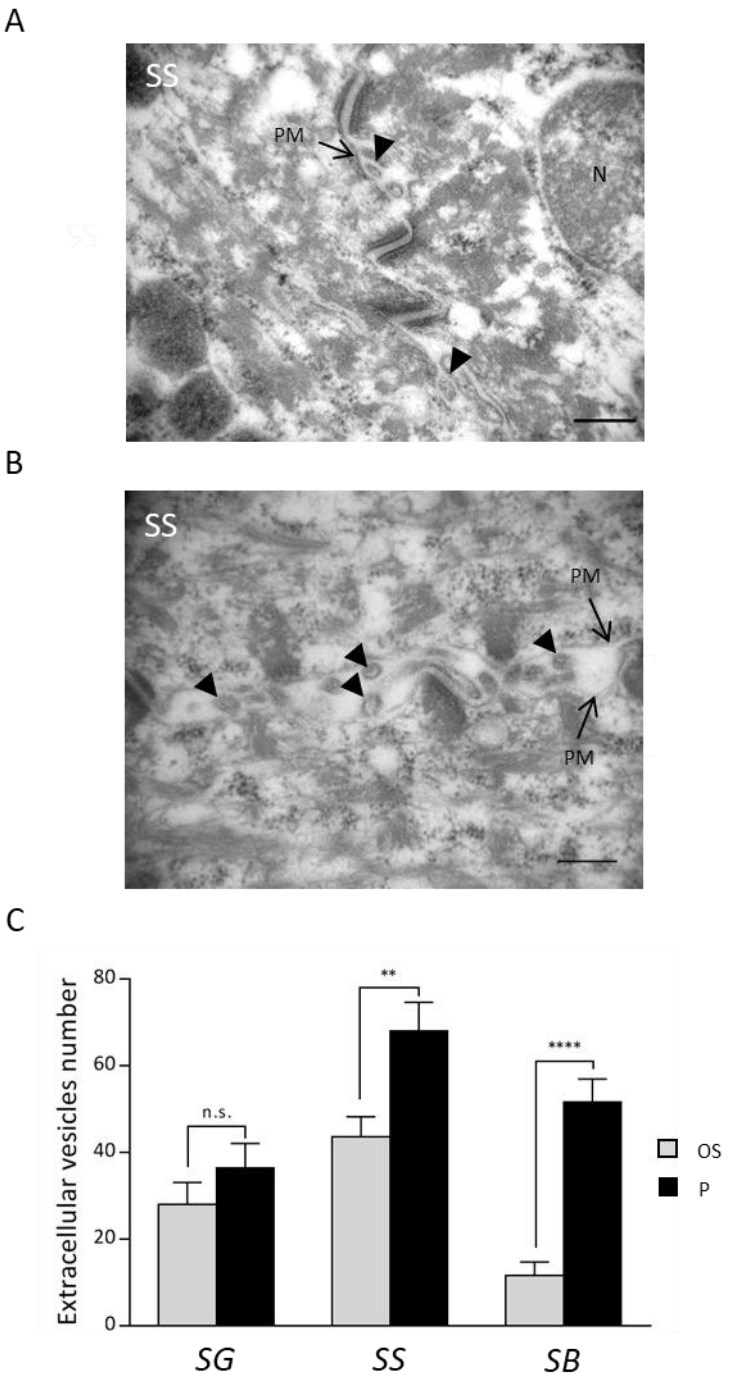

Figure 2: Observation of extracellular vesicle-like structures by transmission electron microscopy (TEM).

Ultrathin sections of skin explants 48h after treatment with OS or P were observed by TEM. Electron micrographs of keratinocytes from *stratum spinosum* after OS (**A**) or P exposure (**B**). Extracellular vesicle-like structures are indicated by black arrowheads. **C**, Quantification of extracellular vesicle-like structures observed by TEM was performed on 10 cells per epidermal layer. **** $P < 0.0001$; ** $P < 0.01$; n.s.: not significant. N: nucleus; OS: organic solvent; P: pollutant mix; PM: plasma membrane; SB: *stratum basale*; SG: *stratum granulosum*; SS: *stratum spinosum.* Scale bars: 250 nm.

Quantification revealed a significant increase of EV-like structures in *stratum spinosum* (SS) and in SB but not in SG after P exposure (Figure 2C). These observations were in line with a study showing that particulate matter exposure can trigger an increase of EV release (Bonzini et al. 2017). Interestingly enough, EVs were found to be involved in tissue remodeling and inflammation modulation in lung after pollutant exposure (Benedikter et al. 2018). Cells release into the extracellular environment diverse types of membrane vesicles that originate from endosomal and plasma membranes called exosomes (30 to 150 nm) and microvesicles/microparticles (100 to 1000 nm), respectively (Raposo and Stoorvogel, 2013). The size of EV-like structures observed in our study was less than 100 nm, suggesting these structures were exosomes, structures discovered in 1985 by Pan et al. (Pan et al. 1985). However, these EV-like structures may also correspond to microvesicles budding from the keratinocyte surface and, in part, to transversally cut cell surface villosities. To define more precisely such EV-like structures, immunolabelling with specific markers should be further performed. The EVs are considered as critical mediators of cell communication (Pleet et al. 2018) regulating several genes in various cell types including dermal fibroblasts (Huang et al. 2015). Recent studies demonstrate that changes of exosomal cargo depend on external stimuli with consequences for the receiving cells (Rokad et al. 2019). Because of their ability to transfer biologically active molecules such as proteins, nucleic acids, and lipids, exosomes play a major role in influencing numerous physiological as well as pathological functions in response to environmental toxicants. These toxicants can be heavy metals (Rokad et al. 2019) as those contained in our P mix.

TEM analysis was also performed on corneocytes previously exposed to diesel particle-enriched solution and collected by tape-stripping (Figure S4 A and B).

~~TEM analysis was also used to observe diesel particles within the explants. First, the upper epidermal layers of explants exposed to diesel particle-enriched solution. and TEM analysis~~

~~was performed on corneocytes collected by tape-stripping (Figure S4).~~ Some dense electron element smaller than 300nm were seen in the corneocytes of exposed explants, while they were absent in corneocytes from explants of the same donor exposed to diesel-free particles solution. ~~Measurements of these particles showed a size of 2.5 nm or smaller~~. Similar ~~particles~~ elements were observed even down to the SG in ultrathin sections of ~~other~~ explants ~~from the same donor~~ 48h after the P nebulization in the Pollubox® (Figure S4 C-F). We hypothesize that these electron dense elements could come from diesel particles. More investigations such as energy dispersive X ray analysis will be necessary to identify them. ~~demonstrating that diesel particles could penetrate the skin explants.~~

3.2 Effect of P on gene expression in cutaneous cells

3.2.1 Gene selection and the functional analysis by PredictSearch®

To evaluate whether our device was indeed efficient to observe the effect of P on HSE at a gene expression level on P-induced relevant targets, a transcriptomic analysis using whole human genome microarrays was performed. Explants generated in triplicate from 4 donors were either left untreated or exposed to P or OS for 1h30 and then maintained in culture for 24h before RNA extraction. Only intensity values higher than background according to Agilent calculations were considered. Fold changes (FCs) were calculated from the ratios between P and OS exposed explants for all triplicates. For each donor and each triplicate, FC$\geq$1.45 and $\leq$0.65 were used to determine up-regulation and down-regulation, respectively. The mean of these FCs among triplicates was then calculated. This selection led to 70 unique up-regulated and 68 unique down-regulated genes (see supplemented data Table S5) common to all 4 donors. The different biological processes and pathways significantly associated with the differentially expressed genes common to all donors were identified using PredictSearch® (Figure 3A and 4B). For each of the terms associated with these processes and pathways, the

enrichment values were calculated (see material and methods) and classified from the highest to the lowest score. Only scores greater than or equal to 2 were considered significant.

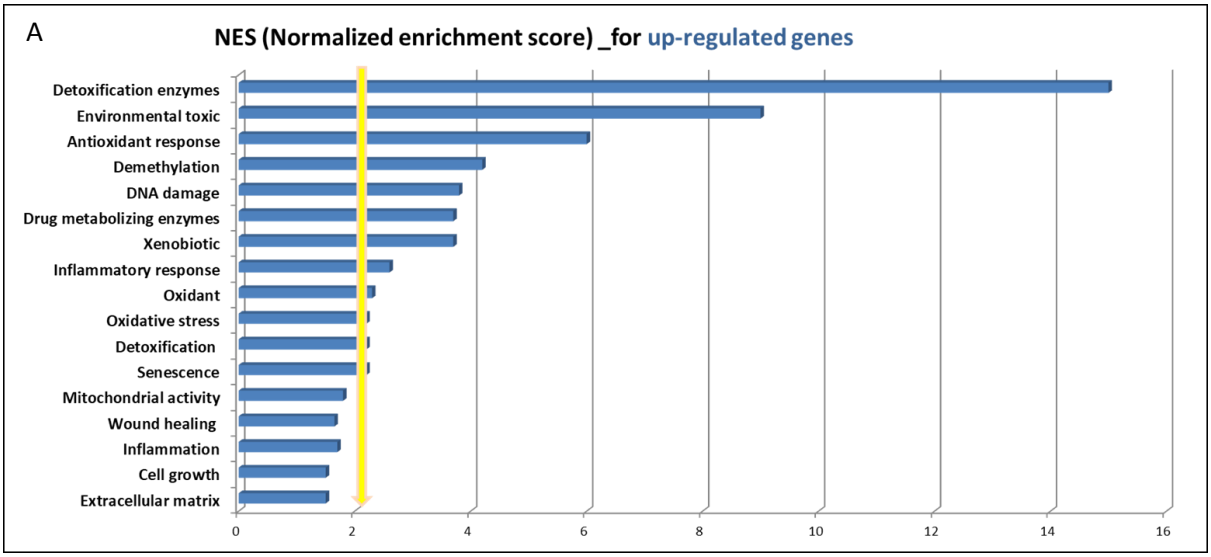

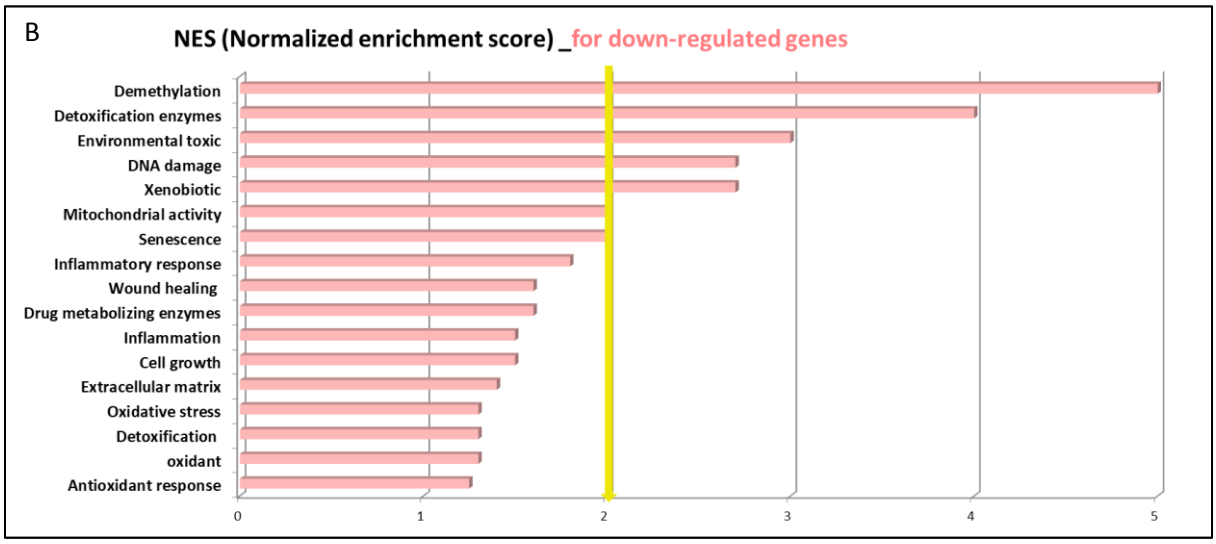

Figure 3: Enrichment of biological terms

Terms related to the selected genes were identified using PredictSearch® software. Classification was achieved according to the normalized enrichment score (NES) as defined in materials and methods. NES exhibiting a value ≥2 are indicated by the yellow arrow. **A**: up-related genes; **B**: Down-regulated genes.

As shown in Figure 3, the term "detoxification enzymes" appeared at the first position for the up-regulated genes (Figure 3A) and at the second position for the down-regulated genes (Figure. 3B). This term was followed by other terms such as "environmental toxic", "DNA damage", "antioxidant response", "xenobiotics" and "demethylation" confirming some of the known effects described upon treatment with pollutants. These results were a confirmation not

only of our experimental design but also of the robustness of our transcriptomic data. Of note, the observation that down-regulated genes shared some terms with up-regulated genes might suggest that at 24h a negative feedback occurred for these specific genes to decrease their expression. For instance, the term "demethylation" might refer, at least in part, to the ability of enzymes such as cytochrome P450 monooxygenases (CYPs) to metabolize drug via N-demethylation (Zanger and Schwab 2012). In addition, epigenetic activities such as DNA methylation are known to be involved in the transcriptional activity of genes encoding enzymes that participate in detoxification and drug metabolism (Zhang et al., 2010). On the other hand, *ALDH5A* and *ALDH7A1* encode enzymes involved in the detoxification of 4-hydroxy-trans-2-nonenal (HNE) implicated in the pathogenesis of numerous neurodegenerative disorders (Murphy et al. 2003), and aldehydes generated by alcohol metabolism and lipid peroxidation (Brocker et al. 2010; Chan et al. 2011), respectively. Mammals have developed oxidative systems that eliminate endogenous and foreign toxic compounds. In humans, this oxidative detoxification depends on the activity of CYPs such as CYP2J2 and CYP4B1. Thus, a repressed expression of these genes might prevent an exacerbation of the response and/or a loss of protection against potential harmful metabolites produced by detoxification. Nevertheless, the functional terms correlated to these genes supported that our device and cultured explants were efficient to elicit a response to pollutants.

3.2.2 Effect of P on the AhR pathway: Xenobiotic responses

Based on the functional correlations found by Predictsearch®, the selected genes were integrated within specific pathways. One of them was related to the AhR–target gene activation. A significant number of genes found modulated by P encoded phase I and II detoxifying enzymes (Figure 4 and Table S4).

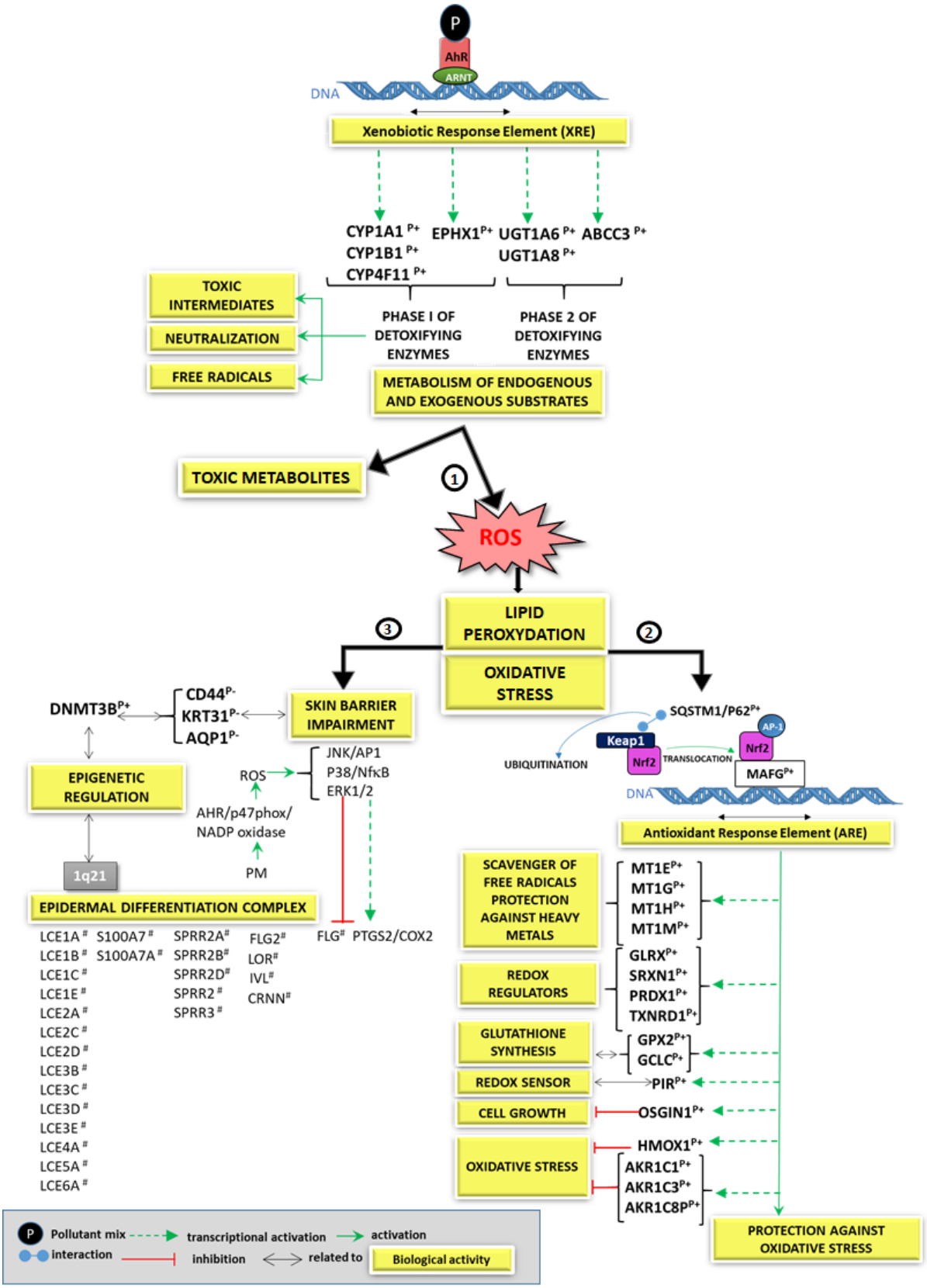

Figure 4: Schematic representation of functional networks deduced from PredictSearch® analysis of the set of genes modulated in HSE 24h after P exposure.

Induced genes or repressed genes are noted by P+ or P- in superscript, respectively. Opposite modulation of skin barrier function-associated genes among volunteers are indicated by # in

superscript. **1**) Genes of the xenobiotic response; **2**) genes of the antioxidant response; **3**) genes related to the skin barrier function.

The AhR is an evolutionarily conserved receptor that is widely expressed in many organs including brain, liver, lung, and skin (Baker et al. 2018; Guastella et al. 2018; Napolitano and Patruno 2018). Once activated by xenobiotic ligands, including dioxin and polycyclic aromatic hydrocarbons, AhR translocates to the nucleus and dimerizes with co-factors including the aryl hydrocarbon receptor nuclear translocator (ARNT), and binds to XREs present in AhR-responsive genes thus increasing their expression (Denison et al. 2011). Interestingly, immunogold analysis on ultrathin sections of skin explants exposed to P compared to OS (Figure S3) showed a significant increase of the nuclear AhR location in granular keratinocytes.

Among the up-regulated genes following P exposure and AhR activation identified by microarrays (Figure 4), the proteins encoded by *CYP1A1* and *CYP1B1* metabolize and detoxify carcinogens, drugs, environmental pollutants and ROS (Başak et al. 2017). *CYP1A1* is expressed by epidermal keratinocytes, dermal fibroblasts, sebaceous glands, hair follicles and subcutaneous striated muscles in normal skin. Other members of the cytochrome family like CYP4F11 whose gene was induced by P, metabolize compounds into irreversible inhibitors of stearoyl CoA desaturase (SCD). SCD is essential to sebocyte development and consequently SCD inhibitors cause skin toxicity (Theodoropoulos et al. 2016). Similarly, induction of genes encoding proteins of phase II (UGT1A6-8 and ABCC3) was also observed in response to P (Table S4). Unlike for CYPs, few studies have demonstrated the expression of *UGT1A6* and especially *UGT1A8* in human skin cells (Diawara et al. 1999; Sumida et al. 2013). Our transcriptomic results showed that the expression of both genes can be induced in HSE after exposure to pollutants and the presence of the corresponding proteins was confirmed by immunostaining in skin explants 48h after P exposure (Figure 5A).

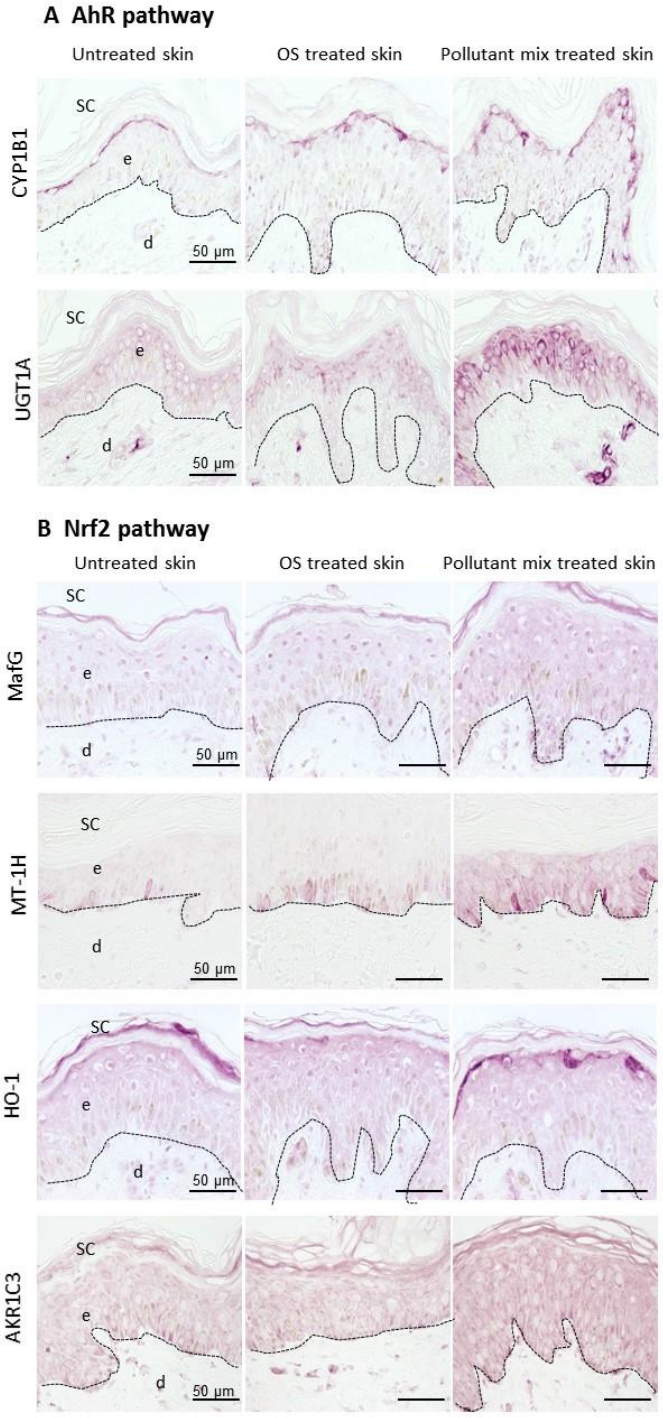

Figure 5: Skin morphology and protein immunolocalization after 48 h following pollutant mix exposure.

Left column: untreated skin samples; central column: skin explants treated with OS; right column: skin explants treated with pollutant mix. For each protein used for immunolabelling, the picture shown in this figure is one representative out of at least 9 images. e: epidermis; d: dermis; OS: organic solvent; SC: *stratum corneum*. Scale bars: 50 µm.

In carcinogenic cells or in liver (Bock and Bock-Hennig 2010; Bock and Köhle 2005), UGTs attenuates the generation of mutagenic benzopyrene metabolites, thus facilitating their detoxification. Accordingly, an induced expression of some of the UGT genes (Figure 4) was observed in our present study. Similarly, the overexpression of one member of the *ABCC* gene family, *ABCC3*, which was described in skin (Osman-Ponchet et al. 2014; Takenaka et al. 2013) was also detected (Figure 4). Genes coding for glutathione/glucuronide sulfate transporters such as ABCC1, ABCC3, and ABCC4 encoding multidrug resistance proteins have been reported to be strongly upregulated during keratinocyte and HaCaT cell differentiation. These proteins are also involved in the translocation of sulfated lipids during SC formation (Kielar et al. 2003). In addition to their role in drug resistance and epidermal lipid layer reorganization, there is substantial evidence that these efflux pumps have overlapping functions in tissue defense and are able to transport a vast and chemically diverse array of toxicants. These toxicants include bulky lipophilic, cationic, anionic, and uncharged drugs and toxins as well as conjugated organic anions that encompass dietary and environmental carcinogens, pesticides, metals, metalloids, and lipid peroxidation products (Leslie et al. 2005).

Related to detoxification processes, *EPHX1* coding for the epoxide hydrolase was also significantly induced by P (Figure 4). EPHX1 is a critical biotransformation enzyme that converts epoxides from the degradation of aromatic compounds to trans-dihydrodiols, which can be conjugated and excreted from the body. Lipid mediators such as arachidonic acid-derived epoxyeicosatrienoic acids, produced by cytochrome P450 epoxygenases, are hydrolyzed by EPHX1 and contribute to tissue growth and wound epithelialization (Edin et al. 2018; Panigrahy et al. 2013).

3.2.3 Effect of P on the NRF2 pathway: Antioxidant responses

The second group of modulated genes illustrated the activation of a NRF2-dependent antioxidant response (Figure5) that follows the production of ROS likely in part generated by CYPs (Table S4). Exposure of cells to xenobiotics, drugs or ionizing radiation is known to generate ROS and electrophiles that lead to oxidative and electrophilic stresses, and has a profound impact on the survival of all living organisms (Kasai 1989; Meneghini 1997). The cells respond to oxidative/electrophilic stresses by activating defense mechanisms that result from the coordinated induction of a battery of genes to protect cells (Dhakshinamoorthy et al. 2000).

The activation of the NRF2 pathway in response to pollutants can be positively regulated by SQSTM1/p62 (Figure 4), which mediates sequestration of Keap1 and promotes translocation of NRF2 to the nucleus (Lau et al. 2013). After translocation, NRF2 forms heterodimers with other transcription factors such as those encoded by genes of the MAF family (*MAFB*, *MAFG*), which bind to ARE, found in promoters of various detoxifying/defensive genes including those described above (Hirotsu et al. 2012; Katsuoka et al. 2005). It should be noted that MAFG immunostaining is significantly enhanced in epidermal cells after P exposure (Figure 5B). *SQSTM1* is also a target gene for NRF2 and creates a positive feedback loop by inducing ARE-driven gene transcription (Jain et al. 2010; Mildenberger et al. 2017).

Among NRF2 target genes, the induction of several members of the metallothionein gene family (*MT1E, MT1H, MT1G*, *MT1M*), which elicited the highest modulation as well as genes involved in antioxidant response (*GPX2, GCLC, HMOX1*) was detected (Figure 4 and Table S4). Among them, the positive modulation in response to P of *MAFG*, *MT-1H* and *HO-1* was confirmed at the protein level by immunohistology (Figure 5B). Metallothioneins are cysteine-rich low molecular weight metal-binding proteins with multiple functions such as cell protection against oxidative stress and heavy metal toxicity as well as the regulated balance of essential metals (Cu and Zn) (Ochiai et al. 2008; Sato and Kondoh 2002).

Glutathione peroxidase 2 (GPX2) catalyzes the reduction of organic hydroperoxides and hydrogen peroxide by glutathione, and thereby protects cells against oxidative damage. The reduction of organic compounds by glutathione can be potentiated through overexpression of a key enzyme encoded by GCLC which contributes to glutathione synthesis.

HMOX1 (HO-1) decreases lipid peroxidation and inhibits the induction of ROS scavenging proteins (Zhang et al. 2012) after an oxidative stress. HMOX1 may also exert anti-inflammatory activities by suppressing the TNF or INF-induced *ICAM1/CD54* expression and subsequent monocyte-keratinocyte adhesion (Seo et al. 2011; Seo et al. 2010) .

Aldo-ketoreductase 1Cs (AKR1Cs) enzymes catalyze the NADPH-dependent reduction of ketosteroids to hydroxysteroids and are members of Phase I metabolizing enzymes involved in the metabolism of steroids (C1-3), prostaglandins (C3), polyaromatic hydrocarbons (C1-3) and xenobiotics (C1-2-4) (Penning and Byrns 2009). They are related to tobacco-carcinogenesis since they activate polycyclic aromatic trans-dihydrodiols to yield reactive and redox active o-quinones. They also detoxify reactive aldehydes derived from exogenous toxicants, e.g., aflatoxin, endogenous toxicants, and those formed from the breakdown of lipid peroxides. *AKRs* are stress-regulated genes and play a central role in the cellular response to osmotic, electrophilic and oxidative stress (Jin and Penning 2007; Palackal et al. 2002). In line with an induced expression of *AKR1C1* and *AKR1C3* genes detected by microarray (Figure 4, Table S4), AKR1C3 was increased at the protein level after P exposure (Figure 5B). In addition to their role in xenobiotic detoxification, AKR1C1 and AKR1C3 are known to elicit an inhibitory effect on oxidative stress (Matsunaga et al. 2013).

3.2.4 Impact of the pollutant mix on the epidermal terminal differentiation complex

Unlike genes of the xenobiotic response, the modulation of the genes located within the epidermal differentiation complex (EDC) locus (Marenholz 2001) was much more heterogeneous among donors (Figure 4, Table S4). Expression of the majority of these genes

was induced in donor V1 and V2, while their expression was mostly unchanged in donor V3 and even reduced in donor V4. It has been reported that particulate matter induces expression of PTGS2/COX2 and represses FLG expression (Lee et al. 2016). These opposite modulations, dependent on AhR signaling and ERK1/2, p38/NF-KB and JNK/AP1 activation, were associated with skin barrier alteration. In our study, while a modulation of *PTGS2/COX2* was not observed, *FLG* expression was effectively suppressed or unchanged in donors V3 and V4, respectively, but induced in donors V1 and V2 (Table S4). In addition to *FLG*, a similar differential pattern among donors was observed with genes encoding FLG2 (filaggrin family member 2), several members of the late cornified envelop protein family (LCE1A, LCE1B, LCE1C, LCE2C, LCE2D, LCE3D, LCE4A, LCE5A and LCE6A), and of the small proline rich protein family (SPRR3, SPRR2A, SPRR2B, SPRR2D, SPRR2G). These genes together with *IVL* (involucrin), *LOR* (loricrin), *CRNN* (cornulin), and *S100A7/PSOR1* (S100 calcium binding protein A7/psoriasin) induced only in donors V1 and V2 belong to the EDC locus on chromosome 1q21.3 (Kypriotou et al. 2012). Genes of this locus encode proteins involved in terminal differentiation and cornification of keratinocytes. To explain such differences between volunteers, it can be suggested that the differentiation follows different kinetics depending on their genetic background or an epigenetic control of gene expression. Indeed, this type of control plays an essential role in regulating stem cell maintenance by repressing the expression of differentiation genes while allowing cell-cycle progression and cell renewal (Goldberg et al. 2007; Spivakov and Fisher 2007).

Local deposition and removal of DNA methylation are tightly coupled with transcription factor binding, although the relationship varies with the specific differentiation process.

A recent study in skin has confirmed a critical role of epigenetic modification for EDC gene transcription (Perdigoto et al. 2014) Therefore, it is possible that the reduced expression of the EDC genes as seen in donors V3 and V4 was donor-dependent under epigenetic control and

contributed to an alteration of the differentiation process and consequently of the skin barrier. It can also be postulated that even in the presence of an efficient activation of a xenobiotic response (equally activated in all 4 donors) to the pollutants, the keratinocyte differentiation process could restore the homeostasis of the cutaneous barrier only later on in donors V3 and V4. Such a difference may rely on a reduced anti-oxidant response illustrated in donors V3 and V4 eliciting a lower expression of *GPX2, AKR1C, AKR1C3, AKR1C8P, HMOX1, SRXN1, PRDX1, TXNRD1, MT1E, MT1H, MT1G and MT1M* (Table S4) when compared to the expression of these genes in donors V1 and V2.

However, repression of some skin integrity key genes such as *AQP1* (aquaporin 1), *CD44* (receptor for hyaluronic acid), and *KRT31* (keratin 31) was observed in all donors (Figure 4, Table S4). This repression might indicate that P treatment compromised cutaneous barrier homeostasis although the recovery to homeostasis might be different among donors. Indeed, it was shown that defective channels like those encoded by aquaporin genes lead to an impaired skin barrier (Blaydon et al. 2014). Moreover, it has been reported that the invalidation of *CD44* in mouse skin leads to a delay in the early barrier recovery following barrier disruption (Bourguignon et al. 2006). In addition, *CD44* downregulation has also been related to inhibited hyaluronan-mediated keratinocyte differentiation. Moreover, the repression of *AQP1* and *CD44* genes was found to be subjected to epigenetic modification as a result of increased methylation by DNMT3 (Smith et al. 2019; Woodson et al. 2006). To investigate the involvement of this process, a methylation profile in HSE upon P treatment will have to be further performed to correlate gene expression and their location within hypo/hypermethylated regions.

Nevertheless, altogether these transcriptomic results supported that our experimental conditions and testing device can evaluate the effects of pollutants on HSE through the modulation of genes of the xenobiotic and anti-oxidant responses as well of EDC genes.

3.2.5 Skin layer-specific response

To gain more insight in the specific response of the different cell layers following P exposure, we isolated by laser capture micro-dissection SB- and SG-enriched fractions from full-thickness explants (Percoco et al., 2012). After RNA extraction from each fraction, RT-qPCR was performed to evaluate the expression of xenobiotic and anti-oxidant response genes. In accordance with microarray and immunohistochemical data, both AhR and NRF2 pathways were modulated (Figure 6). As shown in Figure 6A, P exposure led to a significant increase of these genes in the SB-enriched fraction.

In the SG-enriched fraction (Figure 6B) a significant upregulation for the same genes but to a lesser extent than in the SB-enriched fraction was observed. These data suggested that 24h after P exposure a more efficient transcriptional activity was detectable in the deepest layer of the epidermis than in the granular layer. The response within the deep layers of the epidermis indicated that either some of the pollutant compounds passed through the tissue and/or that the presence of P on the epidermal surface induced a cascade of signaling events from the surface to the deeper layers. Using ^{14}C-labelled benzo[a]pyrene applied on the skin of mice, Yang et al. (1986) showed that hydrocarbons can be recovered in urine, feces and tissues suggesting that these types of pollutants can cross the dermo-epidermal barrier. ~~In contrast, following skin explant exposure in the Pollubox®, we did not detect diesel particles beyond the SG cells.~~ Furthermore, the number of EV-like structures in SS and in SB but not in the SG (Figure 2) suggested also that the deepest layers of the epidermis were able to react to P exposure. While the AhR and NRF2 pathway genes are significantly overexpressed in the SB, the AhR gene was weakly overexpressed or even downregulated in the SG. Interestingly,

detection of AhR receptors in the nucleus of SG cells increased significantly 48h after exposure to P, showing that SG cells were also involved in the P response. It would be interesting to perform these two types of transcriptomic and microscopic analyses at other kinetic points in order to investigate the spatial temporal response of keratinocytes to pollutants.

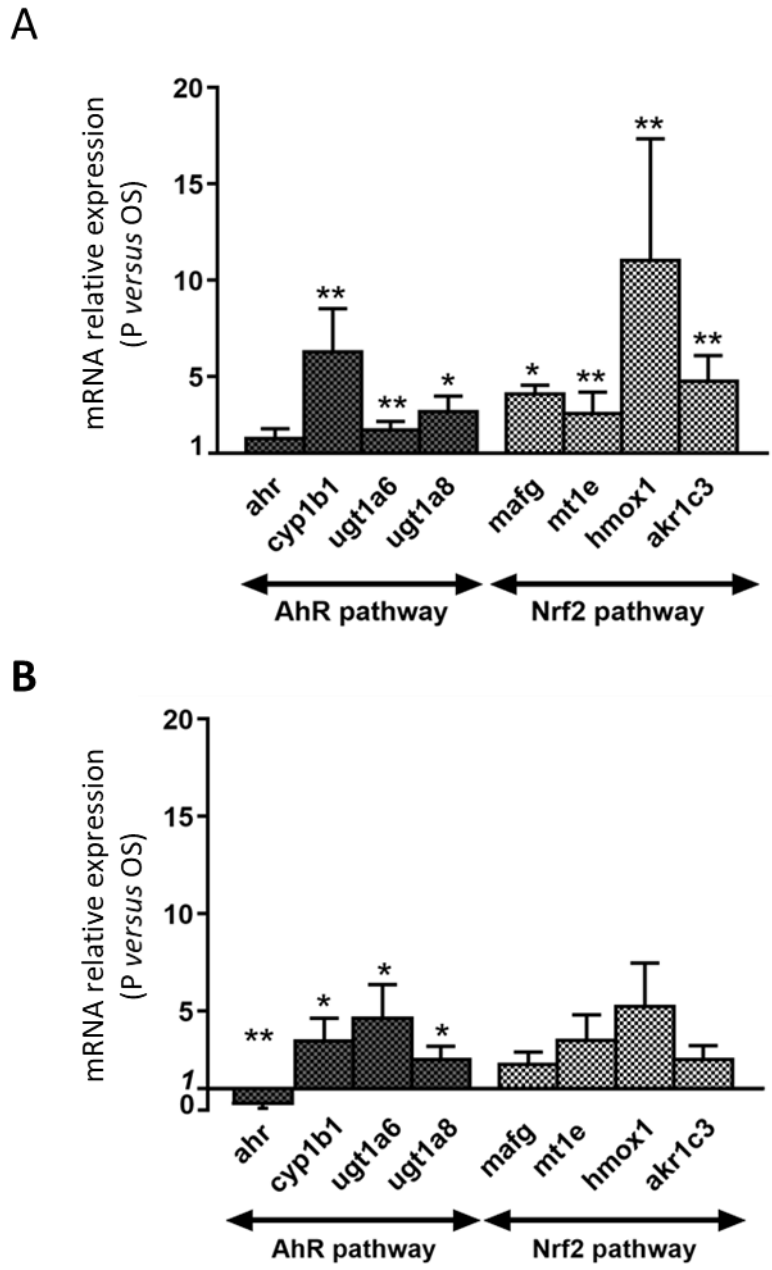

Figure 6: Ratio (P *versus* OS) of gene expression using RNAs extracted from micro-dissected layers of skin explants 24h after P exposure. The ratios of gene expression between P *versus* OS treatment in SB (**A**) and SG (**B**) enriched fractions were determined

with the ΔΔCt method. SB: *stratum basale*; SG: *stratum granulosum*; OS: organic solvents; P: pollutant mix. Mean ± SEM are represented. *$P < 0.1$; **$P < 0.05$ (3 explants each from 4 donors were analyzed).

3. CONCLUSION

Our results demonstrated that efficient xenobiotic and antioxidant responses were triggered in human skin explants exposed in a dedicated chamber to a mix of urban pollutants. Although the dose of each compound contained in the pollutant mixture was far higher than those encountered in a real environment, no morphological alteration of the treated explants (until 48h after exposure) was observed. ~~From our results based on the cutaneous explant model, it can be postulated that diesel particles, smaller than 300 nm, can penetrate the skin down to the granular layer.~~ ~~In contrast,~~ ~~The other~~ Pollutants were able to reach the deepest epidermal layers to modify expression levels of several genes and to increase extracellular vesicle-like secretion. The presence of these vesicles might indicate intensive cross-talk between cells.

Even though no definitive conclusion can be drawn from 4 donors, we found some differences among them between the transcription profiles of genes related to either the xenobiotic/antioxidant responses or the EDC. Most of the genes of the xenobiotic and antioxidant responses were induced in all donors although two donors exhibited a higher induction of these genes than the two others. Interestingly, for these last two donors, no induction (even a repression for one of them) was seen nearly for all the EDC genes while these genes were significantly induced in response to P in the two other donors. Since expression of EDC genes is important for maintaining the skin barrier integrity, the absence of induction or repression of these genes after pollutant exposure might possibly lead to a deleterious effect on terminal differentiation. Such a hypothesis should be investigated further as well as the involvement of individual traits influencing a tissue response to P. Indeed, it can be postulated that the impact of pollutants on terminal differentiation generated by a signal in the deepest layer of the epidermis can vary depending on individual specificities. However, in

order to confirm whether or not gene profiles can be used to assess the skin's ability to resist pollutants and possibly skin aging, explants of more donors should be tested. The comparison of gene expression data with results from microscopic and physico-chemical analyses among donors will have to be systematically performed. Nevertheless, our results demonstrate that these experimental conditions (the P mixture), the tissue model (human skin explants), and the device (Pollubox®) provide a suitable approach to study *ex vivo* the effect of pollutants on skin. This approach can be considered as a new tool to test the potential preventive and/or curative effects of dermo-cosmetic ingredients or end products.

ACKNOWLEDGEMENTS

This work was supported by the 'Fonds Unique Interministériel' (FUI) and 'Le Pôle de compétitivité de la Cosmetic Valley' within the framework of the 'UrbaSkin' project. Images and data were obtained from PRIMACEN: The Cell Imaging Platform of Normandy, from BIO-EC laboratory and from Genex Laboratory. We thank Nabilla Mennad, Antoine Mangin, Laurine Martinelli for help during their training and Claudine Deloménie and Florent Dumont from the UMS IPSIT (Institut Paris Saclay Innovation Thérapeutique) platform for their collaboration. We also thank Anaïs Chamarat, Caroline Durand and Marie Reynier for skin explant preparation and treatment and Cynthia Fays, Tatiana Judith and Ulduz Faradova for their support in skin sample processing for microscopy analysis. The study was conducted in accordance with ethical policies of *Toxicological letters*. The BIO-EC laboratory is authorized by the French Minister for Health to work with biological samples.

AUTHORS CONTRIBUTION

Patatian A, Delestre-Delacour C, Percoco G, Ramdani Y, Di Giovanni M, Bader Th and Bénard M performed the research;

Patatian A, Delestre-Delacour C, Percoco G, Elian E, Benech P and Follet-Gueye ML designed the research study;

Peno-Mazzarino L, Driouich A and Lati E contributed to provide essential reagents and tools;

Patatian A, Delestre-Delacour C, Percoco G, Ramdani Y, Benech P, Follet-Gueye ML analyzed the data;

Patatian A, Delestre-Delacour C, Percoco G, Benech P and Follet-Gueye ML wrote the paper

Benech P and Follet-Gueye ML are the senior co-authors.

REFERENCES

Abel J, Haarmann-Stemmann T. An introduction to the molecular basics of aryl hydrocarbon receptor biology. Biol. Chem. 2010;391(11):1235–48. DOI: 10.1515/BC.2010.128

Addor FAS. Antioxidants in dermatology. An. Bras. Dermatol. 2017;92(3):356–62. DOI: 10.4103/2229-5178.131127

Agren, Jorgensen, Andersen, Viljanto, Gottrup. Matrix metalloproteinase 9 level predicts optimal collagen deposition during early wound repair in humans. Br. J. Surg. 1998;85(1):68–71. DOI: 10.1046/j.1365-2168.1998.00556.x

Baker JR, Gilbert J, Paula S, Zhu X, Sakoff JA, McCluskey A. Dichlorophenylacrylonitriles as AhR Ligands displaying selective breast cancer cytotoxicity in vitro. ChemMedChem. 2018; DOI: 10.1002/cmdc.201800256

Başak K, Başak PY, Doğuç DK, Aylak F, Oğuztüzün S, Bozer BM, et al. Does maternal exposure to artificial food coloring additives increase oxidative stress in the skin of rats? Hum. Exp. Toxicol. 2017;36(10):1023–30. DOI: 10.1177/0960327116678297

Benech PD, Patatian A. From experimental design to functional gene networks: DNA microarray contribution to skin ageing research. Int. J. Cosmet. Sci. 2014;36(6):516–26. DOI: 10.1111/ics.12155

Benedikter BJ, Wouters EFM, Savelkoul PHM, Rohde GGU, Stassen FRM. Extracellular vesicles released in response to respiratory exposures: implications for chronic disease. J. Toxicol. Environ. Health Part B. 2018;21(3):142–60. DOI: 10.1080/10937404.2018.1466380

Binelli A, Magni S, La Porta C, Bini L, Della Torre C, Ascagni M, et al. Cellular pathways affected by carbon nanopowder-benzo(α)pyrene complex in human skin fibroblasts identified by proteomics. Ecotoxicol. Environ. Saf. 2018;160:144–53. DOI: doi: 10.1016/j.ecoenv.2018.05.027

Blaydon DC, Kelsell DP. Defective channels lead to an impaired skin barrier. J Cell Sci. 2014 Oct 15; 127(Pt 20):4343-50 DOI: 10.1242/jcs.154633

Bock KW, Bock-Hennig BS. UDP-glucuronosyltransferases (UGTs): from purification of Ah-receptor-inducible UGT1A6 to coordinate regulation of subsets of CYPs, UGTs, and ABC transporters by nuclear receptors. Drug Metab. Rev. 2010;42(1):6–13. DOI: 10.3109/03602530903205492

Bock KW, Köhle C. UDP-glucuronosyltransferase 1A6: structural, functional, and regulatory aspects. Methods Enzymol. 2005;400:57–75. DOI: 10.1016/S0076-6879(05)00004-2

Bourguignon LY, Ramez M, Gilad E, Singleton PA, Man MQ, Crumrine DA et al. Hyaluronan-CD44 interaction stimulates keratinocyte differentiation, lamellar body formation/secretion, and permeability barrier homeostasis. J Invest Dermatol. 2006;126(6):1356–65. DOI: 10.1038/sj.jid.5700260

Boury-Jamot M, Sougrat R, Tailhardat M, Varlet BL, Bonté F, Dumas M, et al. Expression and function of aquaporins in human skin: Is aquaporin-3 just a glycerol transporter? Biochim. Biophys. Acta BBA - Biomembr. 2006;1758(8):1034–42. DOI: 10.1016/j.bbamem.2006.06.013

Bonzini M, Pergoli L, Cantone L, Hoxha M, Spinazzè A, Del Buono L, et al. Short-term particulate matter exposure induces EV release in overweight subjects. Environ. Res. 2017;155: 228–234. DOI: 10.1016/j.envres.2017.02.014

Brocker C, Lassen N, Estey T, Pappa A, Cantore M, Orlova VV, Chavakis T, Kavanagh KL, Oppermann U, Vasiliou V. Aldehyde dehydrogenase 7A1 (ALDH7A1) is a novel enzyme involved in cellular defense against hyperosmotic stress. J Biol Chem. 2010, Jun 11;285(24):18452-63. DOI: 10.1074/jbc.M109.077925

Carrasco E, Soto-Heredero G, Mittelbrunn M. The Role of Extracellular Vesicles in Cutaneous Remodeling and Hair Follicle Dynamics. Int. J. Mol. Sci. 2019;5;20(11). DOI: 10.3390/ijms20112758

Chan CL, Wong JWY, Wong CP., Chan MKL, Fong WP. Human antiquitin: structural and functional studies. Chem. Biol. Interact. 2011, 191: 165–170. DOI: 10.1016/j.cbi.2010.12.019

Denison MS, Nagy SR. Activation of the Aryl Hydrocarbon Receptor by Structurally Diverse Exogenous and Endogenous Chemicals. Annu. Rev. Pharmacol. Toxicol. 2003;43(1):309–34. DOI: 10.1146/annurev.pharmtox.43.100901.135828

Denison MS, Soshilov AA, He G, DeGroot DE, Zhao B. Exactly the same but different: promiscuity and diversity in the molecular mechanisms of action of the aryl hydrocarbon (dioxin) receptor. Toxicol. Sci. Off. J. Soc. Toxicol. 2011;124(1):1–22. DOI: 10.1093/toxsci/kfr218

Dhakshinamoorthy S, Long DJ, Jaiswal AK. Antioxidant regulation of genes encoding enzymes that detoxify xenobiotics and carcinogens. Curr. Top. Cell. Regul. 2000;36:201–16. DOI: 10.1016/s0070-2137(01)80009-1

Diawara MM, Chavez KJ, Hoyer PB, Williams DE, Dorsch J, Kulkosky P, et al. A novel group of ovarian toxicants: the psoralens. J. Biochem. Mol. Toxicol. 1999;13(3–4):195–203. DOI: 10.1002/(sici)1099-0461(1999)13:3/4<195::aid-jbt10>3.0.co;2-p

Edin ML, Hamedani BG, Gruzdev A, Graves JP, Lih FB, Arbes SJ, et al. Epoxide hydrolase 1 (EPHX1) hydrolyzes epoxyeicosanoids and impairs cardiac recovery after ischemia. J. Biol. Chem. 2018;293(9):3281–92. DOI: 10.1074/jbc.RA117.000298

Estrella B, Naumova EN, Cepeda M, Voortman T, Katsikis PD, Drexhage HA. Effects of Air Pollution on Lung Innate Lymphoid Cells: Review of In Vitro and In Vivo Experimental Studies. Int. J. Environ. Res. Public. Health. 2019;16(13):2347. DOI: 10.3390/ijerph16132347

Eyles D, Almeras L, Benech P, Patatian A, Mackay-Sim A, McGrath J, et al. Developmental vitamin D deficiency alters the expression of genes encoding mitochondrial, cytoskeletal and synaptic proteins in the adult rat brain. J. Steroid Biochem. Mol. Biol. 2007;103(3–5):538–45 DOI: 10.1016/j.jsbmb.2006.12.096

Gasser P, Lati E, Peno-Mazzarino L, Bouzoud D, Allegaert L, Bernaert H. Cocoa polyphenols and their influence on parameters involved in ex vivo skin restructuring. Int. J. Cosmet. Sci. 2008;30(5):339–45 DOI: 10.1111/j.1468-2494.2008.00457.x

Goldberg AD, Allis CD, Bernstein E. Epigenetics: a landscape takes shape. Cell. 2007;128(4):635–8

Guastella AR, Michelhaugh SK, Klinger NV, Fadel HA, Kiousis S, Ali-Fehmi R, et al. Investigation of the aryl hydrocarbon receptor and the intrinsic tumoral component of the kynurenine pathway of tryptophan metabolism in primary brain tumors. J. Neurooncol. 2018; 139(2):239-249. DOI: 10.1007/s11060-018-2869-6

1 Hirabayashi Y. p53-Dependent gene profiling for reactive oxygen species after benzene inhalation:
2 Special reference to genes associated with cell cycle regulation. Chem. Biol. Interact. 2005;153–
3 154:165–70. DOI: 10.1016/j.cbi.2005.03.021

4 Hirotsu Y, Katsuoka F, Funayama R, Nagashima T, Nishida Y, Nakayama K, et al. Nrf2-MafG
5 heterodimers contribute globally to antioxidant and metabolic networks. Nucleic Acids Res.
6 2012;40(20):10228–39. DOI: 10.1093/nar/gks827

7 Huang P, Bi J, Owen GR, Chen W, Rokka A, Koivisto L, et al. Keratinocyte Microvesicles Regulate the
8 Expression of Multiple Genes in Dermal Fibroblasts. J. Invest. Dermatol. 2015;135(12):3051–9. DOI:
9 10.1038/jid.2015.320

10 Iyanagi T. Molecular mechanism of phase I and phase II drug-metabolizing enzymes: implications for
11 detoxification. Int. Rev. Cytol. 2007; 260:35–112. DOI: 10.1016/S0074-7696(06)60002-8

12 Jackson DP, Joshi AD, Elferink CJ. Ah receptor pathway intricacies; signaling through diverse protein
13 partners and DNA-motifs. Toxicol. Res. 2015;4(5):1143–58. DOI: 10.1039/c4tx00236a

14 Jain A, Lamark T, Sjøttem E, Larsen KB, Awuh JA, Øvervatn A, et al. p62/SQSTM1 is a target gene for
15 transcription factor NRF2 and creates a positive feedback loop by inducing antioxidant response
16 element-driven gene transcription. J. Biol. Chem. 2010;285(29):22576–91. DOI:
17 10.1074/jbc.M110.118976

18 Jin Y, Penning TM. Aldo-keto reductases and bioactivation/detoxication. Annu. Rev. Pharmacol.
19 Toxicol. 2007;47:263–92. DOI: 10.1146/annurev.pharmtox.47.120505.105337

20 Jo J-H, Kennedy EA, Kong HH. Topographical and physiological differences of the skin mycobiome in
21 health and disease. Virulence. 2017;8(3):324–33. DOI: 10.1080/21505594.2016.1249093

22 Kasai H. [DNA damage by oxygen radicals and carcinogenesis]. Gan To Kagaku Ryoho. 1989;16(3 Pt
23 2):459–65

24 Katsuoka F, Motohashi H, Engel JD, Yamamoto M. Nrf2 transcriptionally activates the mafG gene
25 through an antioxidant response element. J. Biol. Chem. 2005;280(6):4483–90. DOI:
26 10.1074/jbc.M411451200

27 Kazi T, Arain M, Baig J, Jamali M, Afridi H, Jalbani N, et al. The correlation of arsenic levels in drinking
28 water with the biological samples of skin disorders. Sci. Total Environ. 2008; 407(3):1019-26. DOI:
29 10.1016/j.scitotenv.2008.10.013 2008; Available from:
30 http://linkinghub.elsevier.com/retrieve/pii/S0048969708010425

31 Kielar D, Kaminski WE, Liebisch G, Piehler A, Wenzel JJ, Möhle C, et al. Adenosine Triphosphate
32 Binding Cassette (ABC) Transporters Are Expressed and Regulated During Terminal Keratinocyte
33 Differentiation: A Potential Role for ABCA7 in Epidermal Lipid Reorganization. J. Invest. Dermatol.
34 2003;121(3):465–74. DOI: 10.1046/j.1523-1747.2003.12404.x

35 Kosenko EA, Tikhonova LA, Prakash Reddy V, Aliev G, Kaminsky YG. Differential up-regulation of
36 ammonia detoxifying enzymes in cerebral cortex, cerebellum, hippocampus, striatum and liver in
37 hyperammonemia. CNS Neurol Disord Drug Targets. 2014, 13(6):1089-95, DOI:
38 10.2174/1871527313666140806155929

39 Kurutas EB. The importance of antioxidants which play the role in cellular response against
40 oxidative/nitrosative stress: current state. Nutr. J. 2015;15(1):71. DOI: 10.1186/s12937-016-0186-5

Kypriotou M, Marcel H, Daniel H. The human epidermal differentiation complex: cornified envelope precursors, S100 proteins and the 'fused genes' family. Exp. Dermatol. 2012;21 (9): 643–649. DOI: 10.1111/j.1600-0625.2012.01472.x.

Laghezza Masci V, Taddei AR, Gambellini G, Giorgi F, Fausto AM. Microvesicles shed from fibroblasts act as metalloproteinase carriers in a 3-D collagen matrix. J. Circ. Biomark. 2016;5:1–11. DOI: 10.1177/1849454416663660

Lau A, Whitman SA, Jaramillo MC, Zhang DD. Arsenic-mediated activation of the Nrf2-Keap1 antioxidant pathway. J. Biochem. Mol. Toxicol. 2013;27(2):99–105. DOI: 10.1002/jbt.21463

Lee C-W, Lin Z-C, Hu SC-S, Chiang Y-C, Hsu L-F, Lin Y-C, et al. Urban particulate matter down-regulates filaggrin via COX2 expression/PGE2 production leading to skin barrier dysfunction. Sci. Rep. 2016;6: 6:27995. DOI: 10.1038(1) Available from: http://www.nature.com/articles/srep27995

Leslie EM, Deeley RG, Cole SPC. Multidrug resistance proteins: role of P-glycoprotein, MRP1, MRP2, and BCRP (ABCG2) in tissue defense. Toxicol. Appl. Pharmacol. 2005;204(3):216–37. DOI: 10.1016/j.taap.2004.10.012

Mancebo SE, Wang SQ. Recognizing the impact of ambient air pollution on skin health. J. Eur. Acad. Dermatol. Venereol. 2015;29(12):2326–32. DOI: 10.1111/jdv.13250

Marenholz I. Identification of Human Epidermal Differentiation Complex (EDC)-Encoded Genes by Subtractive Hybridization of Entire YACs to a Gridded Keratinocyte cDNA Library. Genome Res. 2001;11(3):341–55. DOI: 10.1101/gr.114801

Matsunaga T, Hojo A, Yamane Y, Endo S, El-Kabbani O, Hara A. Pathophysiological roles of aldo-keto reductases (AKR1C1 and AKR1C3) in development of cisplatin resistance in human colon cancers. Chem. Biol. Interact. 2013;202(1–3):234–42. DOI: 10.1016/j.cbi.2012.09.024

Meneghini R. Iron homeostasis, oxidative stress, and DNA damage. Free Radic. Biol. Med. 1997;23(5):783–92. DOI: 10.1016/s0891-5849(97)00016-6

Michel L, Reygagne P, Benech P, Jean-Louis F, Scalvino S, So SLK, et al. Study of gene expression alteration in male androgenetic alopecia: evidence of predominant molecular signalling pathways. Br. J. Dermatol. 2017;177(5):1322–36. DOI: 10.1111/bjd.15577

Mildenberger J, Johansson I, Sergin I, Kjøbli E, Damås JK, Razani B, et al. N-3 PUFAs induce inflammatory tolerance by formation of KEAP1-containing SQSTM1/p62-bodies and activation of NFE2L2. Autophagy. 2017;13(10):1664–78. DOI: 10.1080/15548627.2017.1345411

Min-Duk Seo, Tae Jin Kang, Chang Hoon Lee, Ai-Young Lee, and Minsoo Noh. HaCaT Keratinocytes and Primary Epidermal Keratinocytes Have Different Transcriptional Profiles of Cornified Envelope-Associated Genes to T Helper. Cell Cytokines Biomol Ther (Seoul). 2012 Mar; 20(2): 171–176-6 DOI: 10.4062/biomolther.2012.20.2.171

Murphy TC, Amarnath V, Gibson KM, Picklo MJ., Sr. Oxidation of 4-hydroxy-2-nonenal by succinic semialdehyde dehydrogenase (ALDH5A1) J Neurochem. 2003, 86:298–305. DOI.org/10.1046/j.1471-4159.2003.01839.x

Napolitano M, Patruno C. Aryl hydrocarbon receptor (AhR) a possible target for the treatment of skin disease. Med. Hypotheses. 2018;116:96–100. DOI: 10.1016/j.mehy.2018.05.001

Nishimuta H, Sato K, Mizuki Y, Yabuki M, Komuro S. Species differences in intestinal metabolic activities of cytochrome P450 isoforms between cynomolgus monkeys and humans. Drug Metab Pharmacokinet. 2011, Jun;26(3):300-6, DOI: 10.2133/dmpk.DMPK-10-SH-119

Ochiai Y, Kaburagi S, Okano Y, Masaki H, Ichihashi M, Funasaka Y, et al. A Zn(II)-glycine complex suppresses UVB-induced melanin production by stimulating metallothionein expression. Int. J. Cosmet. Sci. 2008;30(2):105–12. DOI: 10.1111/j.1468-2494.2007.00423.x

Osman-Ponchet H, Boulai A, Kouidhi M, Sevin K, Alriquet M, Gaborit A, et al. Characterization of ABC transporters in human skin. Drug Metabol. Drug Interact. 2014;29(2):91–100. DOI: 10.1515/dmdi-2013-0042

Palackal NT, Lee SH, Harvey RG, Blair IA, Penning TM. Activation of Polycyclic Aromatic Hydrocarbon *trans* -Dihydrodiol Proximate Carcinogens by Human Aldo-keto Reductase (AKR1C) Enzymes and Their Functional Overexpression in Human Lung Carcinoma (A549) Cells. J. Biol. Chem. 2002;277(27):24799–808. DOI: 10.1074/jbc.M112424200

Pan BT, Teng K, Wu C, Adam M, Johnstone RM. Electron microscopic evidence for externalization of the transferrin receptor in vesicular form in sheep reticulocytes. J. Cell Biol. 1985;101(3):942–8

Panigrahy D, Kalish BT, Huang S, Bielenberg DR, Le HD, Yang J, et al. Epoxyeicosanoids promote organ and tissue regeneration. Proc. Natl. Acad. Sci. 2013;110(33):13528–33. DOI: 10.1073/pnas.1311565110

Pellerin L, Henry J, Hsu C.Y, Balica S, Jean-Decoster C, Méchin MC. et al. Allergy Defects of filaggrin-like proteins in both lesional and nonlesional atopic skin. Clin. Immunol. 2013; 131(4):1094–102. DOI: 10.1016/j.jaci.2012.12.1566

Penning TM, Byrns MC. Steroid hormone transforming aldo-keto reductases and cancer. Ann. N. Y. Acad. Sci. 2009;1155:33–42. DOI: 10.1111/j.1749-6632.2009.03700.x

Percoco G, Bénard M, Ramdani Y, Lati E, Lefeuvre L, Driouich A, et al. Isolation of human epidermal layers by laser capture microdissection: application to the analysis of gene expression by quantitative real-time PCR. Exp. Dermatol. 2012;21(7):531–4. DOI: 10.1111/j.1600-0625.2012.01509.x

Percoco G, Merle C, Jaouen T, Ramdani Y, Bénard M, Hillion M, et al. Antimicrobial peptides and pro-inflammatory cytokines are differentially regulated across epidermal layers following bacterial stimuli. Exp. Dermatol. 2013;22(12):800–6. DOI: 10.1111/exd.12259

Perdigoto CN, Valdes VJ, Bardot ES, Ezhkova E. Epigenetic regulation of epidermal differentiation. Cold Spring Harb. Perspect. Med. 2014;4(2)

Philips N, Hwang H, Chauhan S, Leonardi D, Gonzalez S. Stimulation of cell proliferation and expression of matrixmetalloproteinase-1 and interluekin-8 genes in dermal fibroblasts by copper. Connect. Tissue Res. 2010;51(3):224–9. DOI: 10.3109/03008200903288431

Pleet ML, Branscome H, DeMarino C, Pinto DO, Zadeh MA, Rodriguez M, et al. Autophagy, EVs, and Infections: A Perfect Question for a Perfect Time. Front. Cell. Infect. Microbiol. 2018;8(362) Available from: https://www.frontiersin.org/article/10.3389/fcimb.2018.00362/full

Rhee SG. Cell signaling. H2O2, a necessary evil for cell signaling. Science, 2006; 312(5782): p. 1882–3. DOI: 10.1126/science.1130481

Raposo G and Stoorvogel W. Extracellular vesicles: exosomes, microvesicles, and friends. J. Cell Biol.. 2013;00(4):373–83

Rokad D, Jin H, Anantharam V, Kanthasamy A, Kanthasamy AG. Exosomes as Mediators of Chemical-Induced Toxicity. Curr. Environ. Health Rep. 2019;6(3):73–9

Rothmiller S, Schröder S, Strobelt R, Wolf M, Wang J, Jiang X, et al. Sulfur mustard resistant keratinocytes obtained elevated glutathione levels and other changes in the antioxidative defense mechanism. Toxicol. Lett. 2018;293:51–61. DOI: 10.1016/j.toxlet.2017.11.024

Seo WY, Goh AR, Ju SM, Song HY, Kwon D-J, Jun J-G, et al. Celastrol induces expression of heme oxygenase-1 through ROS/Nrf2/ARE signaling in the HaCaT cells. Biochem. Biophys. Res. Commun. 2011;407(3):535–40. DOI: 10.1016/j.bbrc.2011.03.053

Seo WY, Ju SM, Song HY, Goh AR, Jun J-G, Kang Y-H, et al. Celastrol suppresses IFN-gamma-induced ICAM-1 expression and subsequent monocyte adhesiveness via the induction of heme oxygenase-1 in the HaCaT cells. Biochem. Biophys. Res. Commun. 2010;398(1):140–5. DOI: 10.1016/j.bbrc.2010.06.053.

Sonoda J, Rosenfeld JM, Xu L, Evans RM, Xie W. A nuclear receptor-mediated xenobiotic response and its implication in drug metabolism and host protection. Curr. Drug. Metab. 2003;4(1):59–72. DOI: 10.2174/1389200033336739

Smith E, Tomita Y, Palethorpe HM, Howell S, Nakhjavani M, Townsend AR, et al. Reduced aquaporin-1 transcript expression in colorectal carcinoma is associated with promoter hypermethylation. Epigenetics. 2019;14(2):158–70, DOI: 10.1080/15592294.2019.1580112

Spivakov M, Fisher AG. Epigenetic signatures of stem-cell identity. Nat. Rev. Genet. 2007;8(4):263–71 DOI: 10.1038/nrg2046

Sumida K, Kawana M, Kouno E, Itoh T, Takano S, Narawa T, et al. Importance of UDP-Glucuronosyltransferase 1A1 Expression in Skin and Its Induction by UVB in Neonatal Hyperbilirubinemia. Mol. Pharmacol. 2013;84(5):679–86. DOI: 10.1124/mol.113.088112

Takenaka S, Itoh T, Fujiwara R. Expression pattern of human ATP-binding cassette transporters in skin. Pharmacol. Res. Perspect. 2013; 1(1): e00005. DOI: 10.1002/prp2.52013;1(1):n/a-n/a

Theodoropoulos PC, Gonzales SS, Winterton SE, Rodriguez-Navas C, McKnight JS, Morlock LK, et al. Discovery of tumor-specific irreversible inhibitors of stearoyl CoA desaturase. Nat. Chem. Biol. 2016;12(4):218–25. DOI: 10.1038/nchembio.2016

WHO report on Exposure to ambient air pollution from particulate matter for 2016 www.who.int/airpollution/data (accessed: April 2018).

Woodson K, O'Reilly KJ, Ward DE, Walter J, Hanson J, Walk EL, et al. CD44 and PTGS2 methylation are independent prognostic markers for biochemical recurrence among prostate cancer patients with clinically localized disease. Epigenetics. 2006;1(4):183–6

Xu J, Yang M, Kosterin P, Salzberg BM, Milovanova TN, Bhopale VM. et al. Carbon monoxide inhalation increases microparticles causing vascular and CNS dysfunction. Toxicol. Appl. Pharmacol. 2013; 273(2): 410–417. DOI: 10.1016/j.taap.2013.09.019

Yang H-L, Lee C-L, Korivi M, Liao J-W, Rajendran P, Wu J-J, et al. Zerumbone protects human skin keratinocytes against UVA-irradiated damages through NRF2 induction. Biochem. Pharmacol. 2018;148:130–46. DOI: 10.1016/j.bcp.2017.12.014

Yang JJ, Roy TA, Mackerer CR. Percutaneous Absorption of Benzo[a]Pyrene in the Rat: Comparison of in Vivo and in Vitro Results. Toxicol. Ind. Health. 1986;2(4):409–16. DOI: 10.1177/074823378600200404

Vierkötter A, Schikowski T, Ranft U, Sugiri D, Matsui M, Krämer U, et al. Airborne Particle Exposure and Extrinsic Skin Aging. J. Invest. Dermatol. 2010;130(12):2719–26. DOI: 10.1038/jid.2010.204

Zanger UM and Schwab M. Cytochrome P450 enzymes in drug metabolism: regulation of gene expression, enzyme activities, and impact of genetic variation. Pharmacol Ther. 2013 Apr;138(1):103-41. DOI: 10.1016/j.pharmthera.2012.12.007

Zhang S, Song C, Zhou J, Xie L, Meng X, Liu P, et al. Amelioration of radiation-induced skin injury by adenovirus-mediated heme oxygenase-1 (HO-1) overexpression in rats. Radiat. Oncol. Lond. Engl. 2012;7:4. DOI: 10.1186/1748-717X-7-4

Zhang D, Ai G, Tanaka H, Hammock BD, Zhu Y. DNA methylation of the promoter of soluble epoxide hydrolase silences its expression by an SP-1-dependent mechanism. Biochim Biophys Acta. 2010 Sep;1799(9):659-67. DOI 10.1016/j.bbagrm.2010.09.006. 0

Zhang Y, Zheng L, Tuo J, Liu Q, Zhang X, Xu Z, et al. Analysis of PM2.5-induced cytotoxicity in human HaCaT cells based on a microfluidic system. Toxicol. Vitro Int. J. Publ. Assoc. BIBRA. 2017;43:1–8. DOI: 10.1016/j.tiv.2017.04.018